Pyrolytic Behavior of Green Macro Algae and Evaluation of Its Activation Energy

S. Daneshvar, F. Salak, and K. Otsuka

***Abstract*—In this research work, the pyrolytic and kinetic characteristics of a green macro algae, Codium Fragile (*C. Fragile*) as a model for marine biomass was studied using thermogravimetric analysis (TGA) method in the range of 313 K to 973 K at atmospheric pressure. Proximate analysis of the freeze dried macro algae showed 6.5% water content, 58% degradable products, 10.5% char, and 25% ash content.**

The influences of particle size, initial weight of the sample, and heating rate on decomposition of the algae have been investigated. Both particle size and initial weight of the sample do not have a significant effect on the TG profile of the algae pyrolysis. In addition, the TGA and DTG (differential thermogravimetric) curves of algae differed significantly for variation in heating rates. The DTG results showed that there are three zones to the pyrolysis; and mainly second zone was significantly affected with heating rates.

The non-isothermic integral isoconventional methods were used to obtain the kinetic parameters from data of the pyrolysis reactions of *C. Fragile* in the second zone. The corresponding activation energies of pyrolysis and decomposition stage of *C. Fragile* were calculated based on the weight loos data obtained from DTG data using the most popular methods (Flynn-Wall-Ozawa (FWO), Kissinger-Akahira-Sunose (KAS), Fredman, and Coast-Redfren methods).

***Index Terms*—Codium Fragile, Green Algae, Kinetic, Marine Biomass, Pyrolysis, Thermogravimetric Analysis**

I. Introduction

The focus on the use of biomass as an alternative feedstock to fossil fuels is intensifying due to its role in reducing CO_2 emissions. Currently many technologies are under investigation for utilization of biomass both for power generation and for production of bio-oil for transportation and chemical commodities [1].

As a consequence there is interest in alternative biomass resources including biomass from an aquatic environment. Marine macroalgae is one such source of aquatic biomass and potentially represents a significant source of renewable energy in coming years. The average photosynthetic efficiency of aquatic biomass is 6–8% [2] which is much higher than terrestrial biomass ones (1.8–2.2%).

Manuscript received July 25, 2012; revised August 26, 2012. This work was supported in part by the Japan Society for the Promotion of Science (JSPS) under Scientific Research Grant (A) 22246110. In addition, Somayeh Daneshvar gratefully acknowledges the JGC-S (Nikki Saneyoshi) Foundation for a scholarship award.

S. Daneshvar and K. Otsuka are with the Department of Marine System Engineering, Osaka Prefecture University, Osaka, JAPAN (e-mail: somayeh@marine.osakafu-u.ac.jp, otsuka@marine.osakafu-u.ac.jp)

F. Salak was with Department of Chemical and Petroleum Engineering, University of Calgary, Calgary, AB, CANADA (f.salak @yahoo.com).

Marine biomass and particularly algae is one of the most widely plant in the world, have variety of industrial applications. They have been reported to contain more than 2400 natural products of commercial importance in pharmaceutical, biomedical, and nutraceutical industries [3].

Those are the main resource materials for phytocolloids such as agar, carrageenan (derived from Rhodophyta) and alginates (derived from Phaeophyta) [4], [5]. The residues from their processing also represent as a feedstock to make renewable fuels.

In fact, there is a great potential for production of bio-chemicals and energy from marine biomass [6].

The methods of conversion into various forms of energy are through several different conversions reactions (chemical, biological, and thermochemical reaction). Among them less attention has been devoted to thermochemical conversions. The different thermochemical options for macroalgae utilization include direct combustion, gasification, pyrolysis and liquefaction.

Pyrolysis as one of the industrially sound process among the thermochemical conversion has been commonly used to convert the different kinds of biomass into bio-oil and bio-char [7]. One of the advanced characterization technique of pyrolysis is thermogravimetric analysis (TGA). TGA is a thermal analysis technique which measures the amount and rate of change in the weight of a material as a function of temperature or time in a controlled atmosphere.

The TGA is used not only for study decomposition kinetics of organic and inorganic compounds, but also widely used for the study of composition of multicomponent systems, oxidative stability of materials, estimated lifetime of a products, the effect of reactive or corrosive atmospheres on materials, moisture and volatiles content of materials [8], [9].

Traditionally, non-isothermal and constant heating rate TGA have been used to obtain kinetic information with the constant heating rate method developed by Flynn and Wall [10] being preferred because it requires less experimental time.

The present study has determined the pyrolysis behavior of *C. Fragile* which selected as model for green macroalgae. This green macroalgae is widely distributed along the shores of East Asia, Oceania, and Northern Europe. In Japan, *C. Fragile* is very familiar seaweed and has been used as a food since ancient times. In addition, its use has been recorded as a treatment for dropsy and dysuria [11], antiangiogenic effect in the prevention of cancer [12] and it shows antiviral activity [13].

We used TGA and DTG techniques in order to evaluate the kinetics of pyrolysis of *C. Fragile*. In addition value of the activation energies were also estimated in various

combustion rates and compared in detail.

II. Experimental

A. Materials

Fresh macroalgae (*C. Fragile*) was collected from Osaka bay near to Rinkou Town Park in Osaka, Japan on 2010. The average water content of *C. Fragile* just after harvesting was found to be 93.3%. Obviously their compositions can vary from batch to batch and by harvesting season [14]. However the remaining solid amount, similar to other marine biomass, is cellulose with some incorporation of hemicelluloses and a wide variety of acidic polysaccharides [15] proteins, lipids, chlorophylls, and other organic and inorganic compounds.

B. Methods

The sample was washed, cleaned of foreign debris, and towel-dried. It was then complete dried using Freeze-drying method (TAITEC freeze dryer VD-16). All the experiments have been performed with initial dry mass close to 20 mg. In fact by freeze drying the moisture content of sample can be reduced to levels acceptable for thermal processing [1].

The dried sample was ground in a laboratory mill MF 10.1 from IKA Works, Inc. USA. It was sieved into six different particle sizes of the sample ranging between <75 and >1400 μm.

Proximate experiments were carried out using a thermogravimetric analyzer (Seiko Exstar 6000 TG/DTA 6300, Seiko Instruments Inc.). Ceramic crucibles were used in order to minimize any thermal lag and to optimize heat transfer between thermocouples and crucibles.

The experiments were performed in an atmospheric pressure and under pure nitrogen gas (99.999%) with flow rate of 20 ml/min. It was performed in non-isothermal condition from room temperature to 973 K.

Pyrolysis was carried out by vary the heating rates from 5 to 50 K/min. The weight losses occurring in correspondence to temperature rises were continuously recorded with a computer working in coordination with the instrument. Effect of particle size (ranging between <75 and >1400 μm) and initial sample weight (ranging between 5-25 mg dry sample) have been studied. Most of the results are presented in TG plot which is plot between weight reduction and temperature. Alternative presentations of results are given as the derivative of the TG or rate of weight reduction against temperature. In this study, all experiments were replicated twice.

III. Kinetic Parameters Estimation

To estimate kinetic parameters, the isoconversional method was used. This method is applied for the description of more complex processes where lots of chemical reactions are running simultaneously; however, their mechanisms are not exactly known [16]. It also has been widely utilized when describing decomposition of biomass [17], [18].

Under non-isothermal conditions in which a sample is heated at constant rate [19], mass loss data from the thermogravimetric analysis can be recalculated into conversion which is defined as follows:

$$\alpha_T = \left(m_{a_0} - m_{aT}\right) / \left(m_{a_0} - m_{a\infty}\right). \quad (1)$$

where m_a is the initial mass of sample, m_{aT} is the mass at temperature T, and $m_{a\infty}$ is final mass of sample at the end of reaction. This method employs a heating rate (β), usually linear, to raise the temperature. A linear heating program follows:

$$T = T_0 + \beta \times t. \quad (2)$$

Here β is the heating rate (K/min) and T is temperature (K) at time t (min).

Under non-isothermal conditions the explicit temperature dependence of the rate equation is given by,

$$d\alpha_T / dT = A / \beta \times e^{-E_a/RT} \times f(\alpha_T). \quad (3)$$

Upon integration of (3) gives

$$g(\alpha_T) = A \Big/ \beta \int_0^T e^{-E_a/RT} dT \quad (4)$$

Which is called the "temperature integral" equation and is the general equation of non-isothermal reaction rate suggested first time by Doyle [20], [21].

In non-isothermal kinetics, the Flynn – Wall – Ozawa (FWO) [22], [10], Kissinger – Akahira – Sunose (KAS) [23-25], Friedman (FR) [26] and Coats-Redfern [27], [28] methods are the most popular representative of the isoconversional methods which used in this study.

IV. Results and Discussion

A. Characteristics of the Thermal Degradation Process on C. Fragile

Fig. 1 illustrates the typical TG profile of *C. Fragile* dehydration, primary devolatilisation, consequently char formation, and finally char oxidation by proximate analysis. Holding freeze dried sample at temperatures below 383 K for 20 min cause to lose weight near 6.5%. This weight loss corresponds to the moisture and cell water content of the sample.

The second weight reduction with temperature rising up to 973 K is attributed to devolatilisation and pyrolysis of mainly natural organic macromolecules. All the volatiles were evolved until 973 K, and only the char remained. In this step, the yield of the volatile material is around 58% of the initial weight of sample. The char content can be found from the oxidation of the produced char by switching the carrier gas from nitrogen to air at 973 K. In this step, the char is oxidized into carbon dioxide and carbon monoxide as well as other gaseous products. The weight differences, before and after switching the gas, was used to determine the fixed carbon, which was about 10.5% of the weight sample. The remaining residue represents the ash content (25%). The ash production of marine biomass is generally higher than grass biomass and lignocellulosic biomass, which is in good coincidence with the fact that marine biomass contains higher salinity [1], [29].

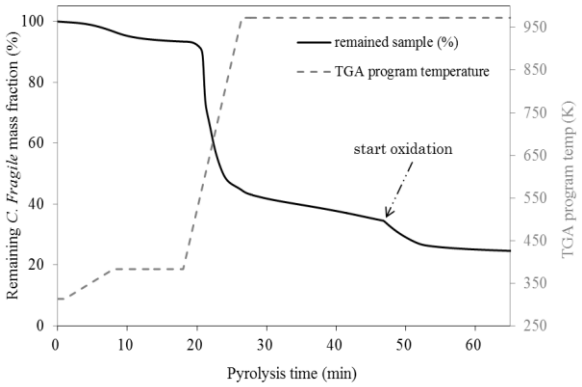

Fig. 1. TG profile for proximate analysis of *C. Fragile* for the particle size of 150~250 μm, 20 mg of initial sample, and heating rate of 50 K/min.

In fact, pyrolysis of *C. Fragile* involving thermal devolatilisation consisted of a very complex set of reactions. The reactions can be represented as the sum of thermal devolatilisation reactions of the individual components of oily compounds, cellulose, hemicellulose, and so on.

Fig. 2 shows typical derivative thermogravimetric (DTG) curve of *C. Fragile* for heating rate of 50 K/min.

This curve indicated that there are three main zones in the pyrolytic process of *C. Fragile*. As it is clear from Fig. 2, the sample revealed large differences in degradation behavior during zone II of the DTG curve. It can be seen that there are three peaks apparent in this zone. The area under the peak represents the weight loss during the reaction. As the temperature increased, the rate of the devolatilisation process also increased.

TABLE I: TEMPERATURES OF INITIAL, PEAK, AND FINAL WEIGHT LOSS OF *C. FRAGILE* SAMPLE OBTAINED FROM DTG CURVES

heating rate, β, (K/min)	Zone I			Zone II									Zone III		
				Stage I			Stage II			Stage III					
	T_i	T_f	T_{max}	T_i	T_f	T_{max}	T_i	T_f	T_{max}	T_i	T_f	T_{max}	T_i	T_f	T_{max}
5	313	358	329	358	435	387	435	558	492	558	648	573	648	973	-
10	313	363	330	363	450	402	450	562	502	562	670	583	670	973	757
20	313	374	334	374	456	415	456	571	516	571	678	597	678	973	758
50	313	415	346	415	490	456	490	603	548	603	723	633	723	973	796

For heating rate of 50 K/min, the first zone occurred as the temperature increased from 313 K to 415 K, while the second zone occurred as the temperature increased from 415 K to 723 K. Zone III started from 723 K and ended at 973 K.

However, these critical temperatures could be varying by heating rate [30]. The corresponding temperatures to each zones and stages as function of heating rates are tabulated in table I. These data was used in this study to distinguish the different zones of each process and their respective reaction kinetics.

Generally, during pyrolysis, the moisture is removed initially at a temperature below 383 K in the zone I [31]. Above 383 K in zone II, the chemical bonds of macromolecules break to release the volatile compounds. Prior to decomposition of macromolecules, oily compounds degrades and evaporate form the sample (zone II, stage I).

At relatively higher temperatures, it has been reported [32] that hemicelluloses degrades fast when compared to cellulose. Above 523 K in stage II, the celluloses may start to break and released more volatiles till up end of the zone II [33].

In zone III, the degradation rate is slow corresponding to the degradation of other less volatile compounds. In fact zone III is the carbonization step and mass loss in this zone can be attributed to char decomposition as well as inorganic ash decomposition and volatilization [29], [1].

B. Effect of Particle Size on Pyrolysis of C. Fragile

The influence of the particle size was investigated for six different particle sizes of the sample ranging between <75 and >1400 μm. Fig. 3 shows only three TGA curves for comparison. As shown, particle size does not have a significant effect on the TG profile of the *C. Fragile* pyrolysis. In contrast, as the particle size increased from 75 to 1400 μm, the char yield decreased somewhat (see Fig. 3 and Table II). This may be due to the amount of heat transfers from different particles size. The samples consisting of larger particle may have had higher rate of heat transfer. As a result, during the second zone, larger amounts of sample were decomposed and less amounts of char remained at the end.

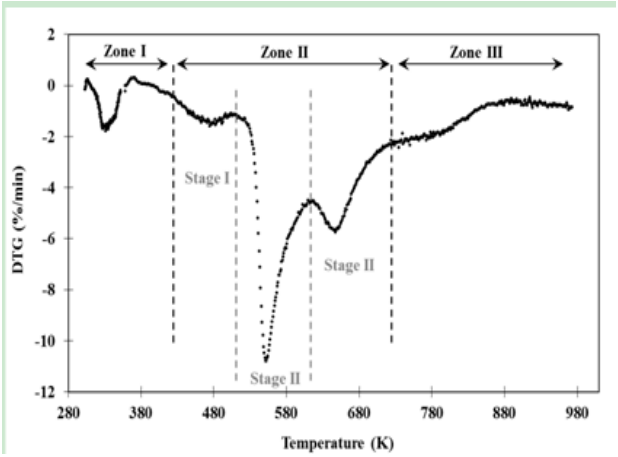

Fig. 2. Typical DTG curve of *C. Fragile* at heating rate of 50 K /min including characteristic temperature zones and stages.

On the other hand, Table II shows as the particle size increased, the ash content decreased somewhat. This might be caused by the effect of heat transfer and diffusion in the bulk of the sample. Heat transfer inside the bulk with larger particles is more efficient compared to the bulk with smaller particles, which produced smaller amounts of ash. Similar results were reported by Mani et al. (2010) [34], Zanzi et al. (2002) [35] and also Chouchene et al. (2010) [36]. In addition, this may be due to the inorganic components separated from the lignocellulosic structure during size reduction of the sample and tend to accumulate in smaller size fractions [37].

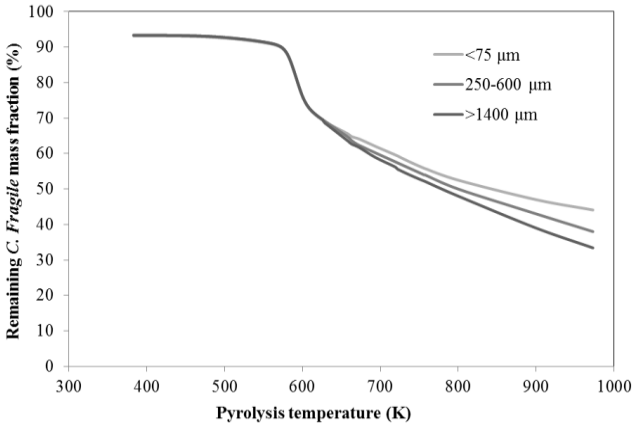

Fig. 3. TG curve of *C. Fragile* at typical different particle sizes with heating rate of 50 K/min and initial sample weight of 20 mg

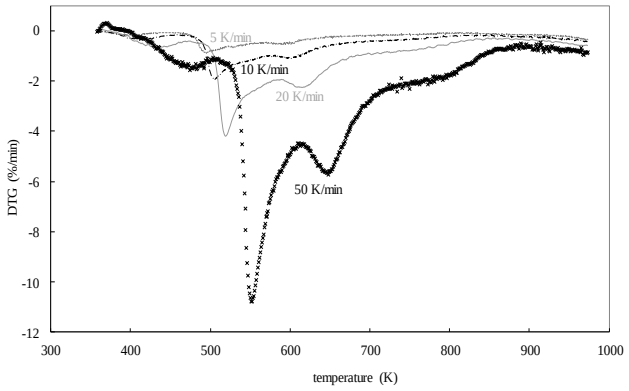

Fig. 4-a. Pyrolysis DTG curves of *C. Fragile* at different heating rates as function of temperature with particle size of 150 ~ 250 µm and initial sample weight of 20 mg

TABLE II: CHAR PERCENTAGE FOR DIFFERENT VALUES OF PARTICLE SIZE OF THE SAMPLE FOR *C. FRAGILE* PYROLYSIS WITH INITIAL WEIGHT 20 MG AND HEATING RATE 50 K/MIN

Ave. particle size (µm)	Char (%)	RSD (%)	Ash content (%)	RSD (%)
≤ 75	11.1	1.7	33.0	1.7
75 ~ 150	10.4	2.1	31.0	0.7
150 ~ 250	10.4	0.7	24.7	0.4
250 ~ 600	10.3	1.2	25.0	0.2
600 ~ 850	9.8	1.8	24.9	0.9
850 ~ 1000	9.9	2.3	24.6	0.8
1000 ~ 1400	9.5	1.8	24.5	0.3
≥ 1400	8.9	2.1	24.5	0.2
Average	**10.0**	-	**26.5**	-

TABLE III: EFFECT OF INITIAL AMOUNT OF THE SAMPLE ON THE CHAR PRODUCTION AT HEATING RATE OF 50 K/MIN AND PARTICLE SIZE OF 150 ~ 250µm

initial sample weight (mg)	Char (%)	RSD %
5	9.3	0.5
10	9.7	0.8
15	10.2	1.2
20	10.4	0.7
25	10.4	0.4
Average	**10.0**	-

C. Effect of Initial Weight on Pyrolysis of C. Fragile

The effect of pyrolysis reaction was studied on initial weight of the *C. Fragile* (Table III). Due to the change of initial amount, TG curves indicated that change in pyrolysis behavior was observed only in the third zone (curves are not shown here). However, initial weight did not have significant effect on the first and the second zones of the pyrolysis of the *C. Fragile*. It was clear that the char yield increased as the initial weight increased. It seems that by increasing the initial weight, the inert gas will encounter a higher diffusion resistance inside the bed. Since the bed sample was getting higher inside the crucible, the heat transfer also would be affected adversely and thus more fixed carbon (char) is produced (see Table III).

D. Effect of Heating Rate on Pyrolysis of C. Fragile

Effect of different heating rates has also been studied for the pyrolysis of *C. Fragile* sample. Fig. 4-a shows the DTG curve and also Fig. 4-b and 4-c show the TG curves of conversions rate at different heating rates from 5 to 50 K/min as function of pyrolysis temperature and time, respectively.

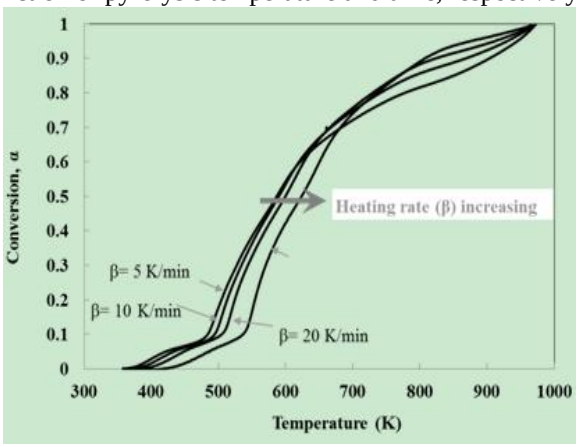

Fig. 4-b. Pyrolysis TGA curves of *C. Fragile* at different heating rates as function of temperature with particle size of 150 ~ 250 µm and initial sample weight of 20 mg

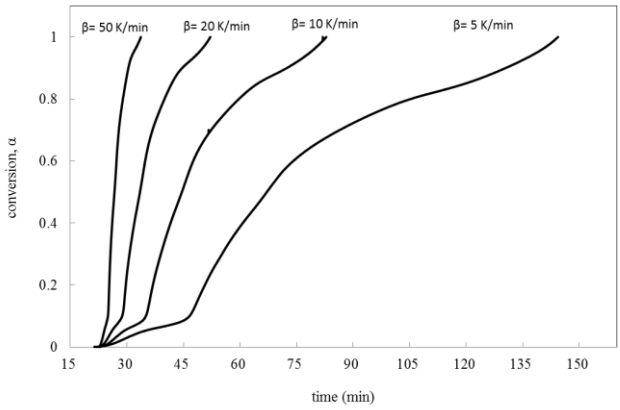

Fig. 4-c. Pyrolysis TGA curves of *C. Fragile* at different heating rates as function of pyrolysis time with particle size of 150 ~ 250 µm and initial sample weight of 20 mg

As shown in Fig. 4 (a-c), there is a shift in conversion lines caused by various heating rates. At higher heating rates, individual conversions are reached at higher temperatures. In other word at higher heating rates, higher temperatures are required to achieve the same conversion level [16], [38].

The maximums of the decomposition rate are also slightly shifted towards higher temperatures. This fact can be a consequence of heat and mass transfer limitations. It means that temperature in the furnace space can be a little higher as the temperature of particle, and the rate of devolatilization is higher than the release of volatilities. Because of the heat transfer limitation, temperature gradients may exist in the particle. Temperature in the core of a particle can be a bit

lower than temperature on the surface, and different devolatilization processes or releasing rates can occur. This is the reason, why it is necessary to have a small particle, homogenous sample and heat transfer surface between the sample and the crucible as large as possible [16].

At higher heating rate, the devolatilisation process occurred sooner due to the increased rate of heat transfer between the crucible and the sample (Fig. 4-c). Faster heating rates cause the primary devolatilisation to complete rapidly because the temperature for secondary devolatilisation has been reached rapidly. Since the faster heating rate led to less efficient heat transfer, the devolatilisation rate increase faster than at lower heating rates, thus shifting the peak of the devolatilisation rate.

Meanwhile, as the heating rate increased the ash yield increased. At the lower heating rate, the heat transfer between the crucible and the sample were more efficient. This resulted in a proper drying and devolatilisation during the first and second zones, respectively. As a result, char yield increased as the heating rates increased, as shown in Table IV.

TABLE IV: CHAR YIELD FOR DIFFERENT VALUES OF HEATING RATE IN PARALYSIS OF *C. FRAGILE* WITH AVERAGE PARTICLE SIZE 150 ~ 250μm AND INITIAL WEIGHT 20MG

Heating rate, β, (K/min)	Char %	RSD %
5	8.7	1.3
10	9.3	0.7
20	9.5	0.2
50	10.2	0.2

E. Kinetic Analysis of the Pyrolysis Process for C. Fragile

1) Assumptions:

(1) The pyrolysis process was assumed to take place in three zones (see Fig. 2). Since zone II is the main step of pyrolysis process, therefore, the three stages of *C. Fragile* pyrolysis in the zone II was only chosen for kinetic studies. The temperatures selected to distinguish between stages of the zone II are shown in Table I.

(2) The moisture and adsorbed water content released up to 383 K was excluded from pyrolysis data.

(3) All the pyrolysis retractions assumed to be irreversible ones [39].

(4) Since it is impossible to identify all the compounds in the pyrolysis of *C. Fragile*, the model is based on only weight loss.

(5) Simple solid-state pyrolysis reaction model was assumed for *C. Fragile* sample. To estimate kinetic parameters, the isoconversional methods were used.

(6) Among the several approximated analytical solution methods, the most common methods were selected to calculate the activation energy of the pyrolysis of *C. Fragile*.

(7) The effects of the internal mass transport as a significant resistance inside the particles during pyrolysis are not considered in this study.

2) Approximated analytical solutions of the rate equation for C. Fragile pyrolysis:

The experimental data were processed in order to obtain activation energies [16]. Predefined conversions were in the range from 0.05 to 0.7. From the set of data at different heating rates (5, 10, 20, and 50 K/min), the isoconversional lines for predefined conversion were calculated. Because at higher temperatures no significant changes occur in conversion, the isoconversional lines were not very precise.

Different heating rates give different Arrhenius plots; therefore a series of E_a values can be determined from the slopes of the each isoconversional straight lines at conversion degrees (α). The pre-exponential factor can be obtained from the intercept of the isoconversional line.

a) Ozawa, flynn and wall (OFW) method

Ozawa, Flynn and Wall (OFW) method [22], [40] is one of the non-isothermal methods which used to determine the energy of activation (E_a) at constant several conversion degrees (α). This method is based on the following equation:

$$\ln \beta = \ln\left(A0.0048AE_a / Rg(\alpha)\right) - 1.0516\,E_a / RT. \quad (5)$$

For α= constant, ln(β) versus 1/T obtained at several heating rates yields a straight line whose slope allows evaluation of the apparent activation energy [38].

Fig. 5 shows the Arrhenius plots of ln(β) versus l/T at constant conversions but different heating rates. The activation energies (E_a) determined from the slope of each line along with line equations and R- square values calculated by FOW method for each α are listed in Table V. R-squared values show good fitting of the straight lines obtained by FOW method. Therefore, it can be concluded that activation energies calculated by FOW methods are valid [30].

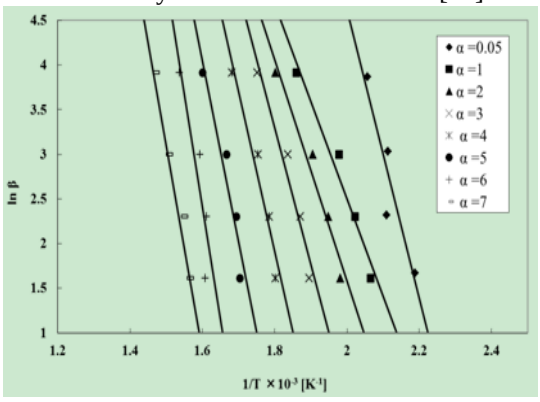

Fig. 5. FOW plots of *C. Fragile* at different conversion fractions

b) The method of Friedman

This method [26] was one of the earliest isoconversional methods, which according to the non-isothermal rate law gives,

$$\ln\left(\beta\, d\alpha/dt\right) = \ln\left(A_\alpha f(\alpha)\right) - E_a / RT. \quad (6)$$

TABLE V: ACTIVATION ENERGIES CALCULATED BY FOW METHOD

α_T	Curve fit equatuion	R-Squared value	E_a (/kJmol^{-1})
0.05	y = -16.1x + 36.909	0.86	293.9
0.1	y = -10.9x + 24.313	0.96	198.5
0.2	y = -12.4x + 26.39	0.96	225.7
0.3	y = -15.3x + 30.854	0.95	278.6
0.4	y = -17.9x + 34.143	0.94	325.9
0.5	y = -20.2x + 36.44	0.91	368.5
0.6	y = -25.2x + 42.737	0.80	458.9
0.7	y = -22.9x + 37.483	0.98	417.3

Hence, a plot of ln [βdα/dt] versus 1/T at each conversion degree (α_T) gives activation energy E_a from the slope of the plot. The constructed plots are shown in Fig 6. The activation energies (E_a) along with line equations and R- square values calculated by Friedman method for each α are listed in Table VI.

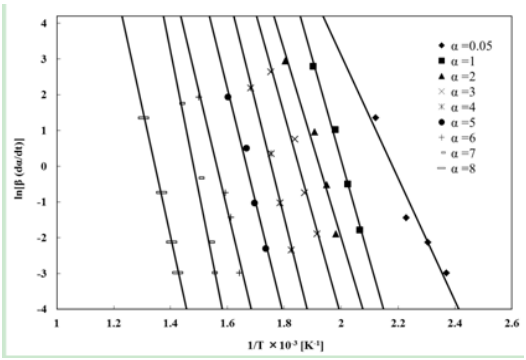

Fig. 6. Friedman plots of *C. Fragile* at different conversion fractions

TABLE VI: ACTIVATION ENERGIES CALCULATED BY FRIEDMAN METHOD

α_T	Curve fit equation	R-Squared value	E_a (/kJmol^{-1})
0.05	y = -28.0x + 56.232	0.99	233.1
0.1	y = -17.2x + 37.495	0.94	142.9
0.2	y = -26.2x + 50.464	0.96	218.0
0.3	y = -28.2x + 52.217	0.98	234.6
0.4	y = -31.8x + 55.83	0.98	264.5
0.5	y = -32.2x + 53.65	0.97	267.5
0.6	y = -33.1x + 51.743	0.98	275.3
0.7	y = -39.7x + 58.797	0.97	329.9
0.8	y = -36.2x + 48.732	0.99	301.1

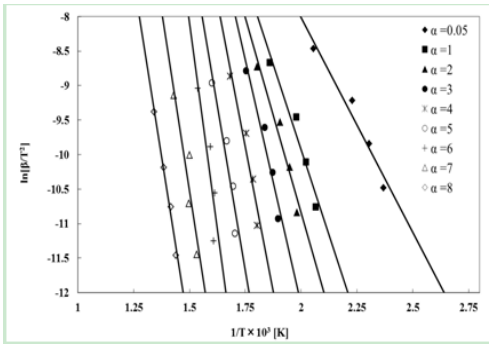

Fig. 7. KAS plots of *C. Fragile* at different conversion fraction

c) Kissinge-akahira-SUNOSE (KAS) method

The Kissinger-Akahira-Sunose (KAS) method [24], [25] was based on the following equation,

$$\ln\left(\beta/T_\alpha^2\right)=\ln\left(AR/E_a g(\alpha)\right)-E_a/RT. \quad (7)$$

The activation energies (E_a) can be determine from the linear plots of the $\ln\beta/T^2$ versus 1/T temperature corresponding to each conversion degree (Fig. 7). Same as the other methods the activation energies can be determined without a precise knowledge of the reaction mechanism. The activation energies (E_a) along with line equations and R-square values calculated by KAS method for each α are listed in Table VII.

d) The method of coast-redfern

This method [27], [28] is a non-isothermal model free method and uses the integral form of the non-isothermal rate

TABLE VII: ACTIVATION ENERGIES CALCULATED BY KAS METHOD

α_T	Curve fit Eq.	R-Squared value	E_a (/kJmol^{-1})
0.05	y = -9.9x + 9.8623	0.96	82.3
0.1	y = -6.2x + 4.4282	0.95	51.7
0.2	y = -11.3x + 11.843	0.95	94.3
0.3	y = -14.2x + 16.235	0.94	118.1
0.4	y = -16.7x + 19.433	0.93	139.3
0.5	y = -19.0x + 21.625	0.9	158.2
0.6	y = -23.9x + 27.827	0.78	199.0
0.7	y = -20.9x + 20.766	0.86	173.455
0.8	y = -20.4x + 18.042	0.99	169.7

law which gives,

$$\log\left(-\log(1-\alpha)^{(1-n)}/T^2(1-n)\right)= \log AR/\beta E_a\left(1-2RT/E_a\right)-E_a/2.3RT. \quad (8)$$

The left-hand side of (8) versus 1/T was plotted and the slope of these lines gave the E_a values. In the present study, the orders 0.5, 1, and 1.5 were plotted for (8) and the best correlation coefficients were obtained for n= 1. The straight line plots for *C. Fragile* are given in Figs. 8 (a-d), and the calculated activation energies are cited in Table VIII (and for comparison in Fig. 9)

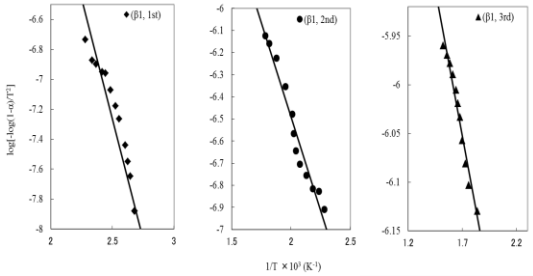

Fig. 8-a. Coats-redfern plots of *C. Fragile* (with average particle size 150 ~ 250 μm, heating rate 5 min–1) for stages I, II, and III.

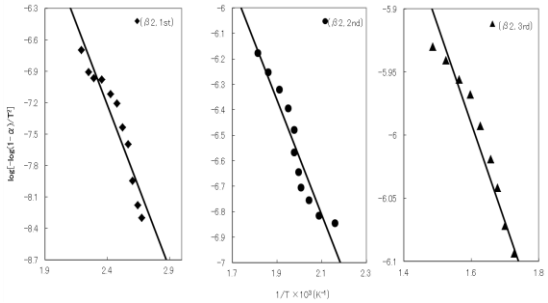

Fig. 8-b. Coats-redfern plots of *C. Fragile* (with average particle size 150 ~ 250 μm, heating rate 10 min–1) for stages I, II, and III.

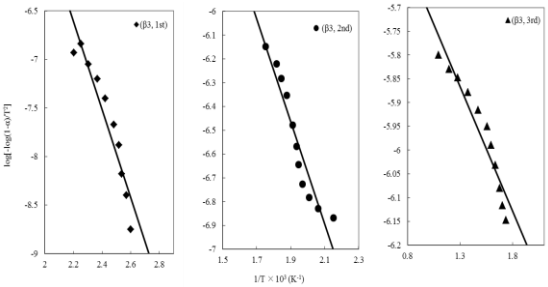

Fig. 8-c. Coats-redfern plots of *C. Fragile* (with average particle size 150 ~ 250 μm, heating rate 20 min–1) for stages I, II, and III.

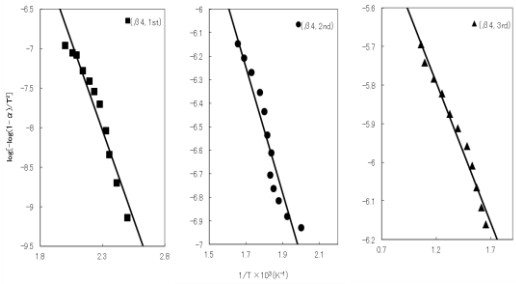

Fig. 8-d. Coats-redfern plots of *C. Fragile* (with average particle size 150 ~ 250 μm, heating rate 50 min–1) for stages I, II, and III.

TABLE VIII: ACTIVATION ENERGIES CALCULATED USING COATS-REDFERN METHOD FOR EACH STAGE AS FUNCTION OF HEATING RATE

Heating rate	Stage	Curve fit equation	R-Squared value	E_a (/kJmol^{-1})
β1 5 K/min	I	y = -3.2x + 0.7771	0.95	61.6
	II	y = -1.7x - 3.0866	0.96	32.6
	III	y = -0.6x - 5.0234	0.97	11.6
β2 10 K/min	I	y = -3.1x + 0.2596	0.90	59.7
	II	y = -2.3x - 2.0583	0.91	43.3
	III	y = -0.7x - 4.7433	0.95	14.9
β3 20 K/min	I	y = -4.5x + 3.3629	0.9	86.8
	II	y = -2.1x - 2.3732	0.91	41.2
	III	y = -0.5x - 5.185	0.91	10.0
β4 50 K/min	I	y = -4.5x + 2.3154	0.94	86.2
	II	y = -2.7x - 1.6937	0.91	51.3
	III	y = -0.7x - 4.9175	0.97	13.9

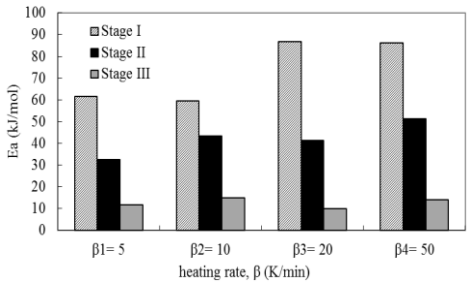

Fig. 9. Activation energies calculated from Coats-Redfern method for each stage

3) Comparison of activation energies from different methods

Table IX listed the activation energies calculated by different methods for each conversion fraction as well as each stage. The average activation energies were also calculated for each stage. The average values of E_a in the range 0.05 to 0.1 of (stage I) were 73.4, 67.0, 188.0, and 218.7 kJ/mol, in the range 0.2 to 0.6 (stage II) were 42.1, 141.8, 251.9, and 331.5 kJ/mol, and the average values of E_a in the range 0.7 to 0.8 (stage III) were 12.6, 171.5, 315.4, and 417.3 kJ/mol which obtained for each stage by Coast-Redfren, KAS, Friedman, and FOW methods, respectively.

The activation energies calculated by FOW and Friedman methods for each three stages are higher than those using KAS and Coats-Redfern methods, it can be said that the results are fairly compatible with each other [41]. The values of the apparent activation energies obtained by Coast-Redfren method are lower than that of FWO, Fredmean, and KAS methods [19].

The data show that energy of activation dependent of conversion (see Table IX) and the apparent activation energy sharply increase with increase in the degree of conversion for FOW, Friedman, and KAS methods.

V. CONCLUSION

The thermal decomposition of *C. Fragile* was investigated in detail. In the present study we assume that the activation energy is a function of conversion. In fact, the value of the activation energy can give an idea about the optimum reaction conditions in process chemistry, it gives an idea about the thermal stability and the expected lifetime of a compound to be kept at a certain temperature or it provides information in quality research [42].

We have realized that pyrolysis of seaweed can be influenced by the pyrolysis temperature, particle size, and heating rate. Therefore, it is necessary to evaluate all these parameters for any type of marine biomass prior to scale up the pyrolysis system.

The integral methods which use the approximations of the temperature integral are generally reliable methods for the calculation of activation energies of thermally stimulated reactions studied during linear heating. Activation energies for three pyrolysis stages of *C. Fragile* were obtained with the methods of Ozawa, Flynn and Wall (OFW), Kissinger-Akahira-Sunose, and Coats-Redfern.

At higher conversions, the activation energy started increasing rapidly as the whole process slowed down.

TABLE IX: ACTIVATION ENERGIES CORRESPONDING TO THE DECOMPOSITION OF *C. FRAGILE* FOR EACH CONVERSION AND EACH STAGE; CALCULATED BASED ON FOUR METHODS: FWO, FRIEDMAN, KAS, AND COAST-REDFREN

	stage	I		II					III	
	α	0.05	0.1	0.2	0.3	0.4	0.5	0.6	0.7	0.8
FOW	$E_{a(\alpha)}$	293.9	198.5	225.7	278.6	325.9	368.5	458.9	417.3	-
	E_a (ave)	218.7				331.5			417.3	
Friedman	$E_{a(\alpha)}$	233.1	142.9	218.0	234.6	264.5	267.5	275.3	329.9	301.0
	E_a (ave)	188.0				251.9			315.4	
KAS	$E_{a(\alpha)}$	82.3	51.7	94.3	118.1	139.3	158.2	199.0	173.4	169.7
	E_a (ave)	67.0				141.8			171.5	
Coast-Redfren	$E_{a(\alpha)}$	-	-	-	-	-	-	-	-	-
	E_a (ave)	73.4				42.1			12.6	

REFERENCES

[1] A. B. Ross, J. M. Jones, M.. L. Kubacki, and T. Bridgeman, "Classification of macroalgae as fuel and its thermochemical behavior," *Bioresource Technology*, vol. 99, pp. 6494–6504, 2008

[2] Renewable biological systems for alternative sustainable energy production, *Food and Agriculture Organization of the United Nations (FAO)*, Agricultural Services Bulletin – 128, 1997.

[3] M. H. G. Munro, J. W. Blunt, *Marinlit*, Mar. Chem. Group, Univ. of Canterbury, Christchurch, New Zealand, vol. 10. 4, 1999.

[4] I. A. Abbott, "Seaweeds and their uses," *Aquatic Botany 12*, pp. 389–390, 1982.
[5] G. C. Cade ́e, "Seaweed resources in Europe: uses and potential," *Aquaculture*, vol. 107, no. 4, pp. 395–396, 1992.
[6] W. Peng, Q. Wu, and P. Tu, "Effects of temperature and holding time on production of renewable fuels from pyrolysis of Chlorella protothecoides," *Journal of Applied Phycology*, vol. 12, no. 2, pp. 147-152, 2000.
[7] N. Mahinpey, P. Murugan, T. Mani, and R. Raina, "Analysis of bio-oil, bio-gas and bio-char from pressurized pyrolysis of wheat straw using a tubular reactor," *Energy Fuels*, vol. 23, no. 5, pp. 2736–2742, 2009.
[8] P. S. Gill, S. R. Sauerbrunn, and B. S. Crowe, J. Therm. Anal. vol. 38, pp. 255-266, 1992.
[9] "TA Instruments Application Brief TA-125," Zsako, and Zsako, *J. Therm. Anal*, vol. 19, no. 33, 1980.
[10] Flynn and Wall, *Polymer Letter*, vol. 19, pp. 323, 1966.
[11] J. B. Lee, Y. Ohta, K. Hayashi, and T. Hayashi, "Immunostimulating effects of a sulfated galactan from Codium fragile," *Carbohydr. Res.* pp. 1452, 2010.
[12] P. Ganesan, K. Matsubara, T. Ohkubo, Y. Tanaka, K. Noda, T. Sugawara, and T. Hirata, "Anti-angiogenic effect of siphonaxanthin from green alga, Codium fragile," *Phytomedicine*, vol. 17, pp. 1140, 2010.
[13] Y. Ohta, J. B. Lee, K. Hayashi, and T. Hayashi, "Isolation of sulfated galactan from Codium fragile and its antiviral effect," *Biol. Pharm. Bull*, vol. 32, no. 5, pp. 892, 2009
[14] E. M. Soriano, P. C. Fonseca, M. A. A. Carneiro, W. S. C. Moreira, "Seasonal variation in the chemical composition of two tropical seaweeds," *Bioresource Technology*, vol. 18, pp. 2402–2406, 2006.
[15] W. F. Dudman, "Detection of acidic polysaccharides in gels by DEAE-dextran," Anal. Biochem, vol. 46, no. 2, pp. 668, 1972.
[16] L. Gašparovič, Z. Koreňová, and L. Jelemensk ý1, "Kinetic study of wood chips decomposition by TGA," 36th International Conference of SSCHE, Tatransk é Matliare, Slovakia, May 25–29, 2009.
[17] Y. H. Park, J. Kim, S.S. Kim, and Y. K. Park., "Pyrolysis characteristics and kinetics of oak trees using thermogravimetric analyzer and micro-tubing reactor," *Bioresource Technology*, vol. 100, no. 1, pp. 400-405, 2009.
[18] E. Biagini, A. Fantei, and L. Tognotti, "Effect of the heating rate on the devolatilization of biomass residues," *Thermochimica Acta*, vol. 472, pp. 1-2, pp. 55-63, 2008.
[19] M. Vennila, G. Manikandan, V. Thanikachalam, and J. Jayabharathi, "Thermal decomposition of N-(salicylidene)L- leucine in static air atmosphere," European Journal of Chemistry, vol. 2, no. 2, pp. 229-234, 2011.
[20] C. D. Doyle, "Kinetic analysis of thermogravimetric data," J. App. Polym. Sci, vol. 5, pp. 285-292, 1961.
[21] C. D. Doyle, "Quantitative calculations in thermogravimetric analysis," in Slade, P. E., jr.; Jenkins, L. T. (Eds.): Techniques and methods of polymer evaluation I. New York: Marcel Dekker, Inc, 1966, pp. 113 211.
[22] T. Ozawa, "new method of analyzing thermogravimetric data," Bull. Chem. Soc. Jpn, vol. 38, pp. 1881-1886, 1965.
[23] K. Slopiecka, P. Bartocci, and F. Fantozzi, "Thermogravimetric analysis and Kinetic study of poplar wood pyrolysis," 3*rd Inter. Conf. on Applied Energy*, Perugia, Italy, 16-18 May 2011, pp. 1687-1698.
[24] H. Kissinger, "Variation of peak temperature with heating rate in differential thermal analysis," *Journal of Research of the National Bureau of Standards*, vol.57, no. 4, pp. 217-221, 1956.
[25] T. Akahira and T. Sunose, "Joint convention of four electrical institutes," *Science Technology*, vol.16, pp. 22–31, 1971.
[26] H. L. Friedman, and J. Polym, *Sci. Polym. Lett*, 6C, pp. 183-195. 1963.
[27] A. W. Coats and J. P. Redfern, "Kinetic Parameters from Thermogravimetric Data," Nature, vol. 201, pp. 68-69, 1964.
[28] A. W. Coats, and J. P. Redfern, J. Polym. Sci., Part B: Polym. Lett., vol. 3, pp. 917-920, 1965.
[29] Z. Hui, Y. Huaxiao, Z. Mengmeng, and Q. Song, "Pyrolysis Characteristics and Kinetics of Macroalgae Biomass Using Thermogravimetric Analyzer," World Academy of Science, Engineering and Technology, vol. 65, pp. 1161-1166, 2010.
[30] N. Ye, D. Li, L. Chen, X. Zhang, and D. Xu, "Comparative Studies of the Pyrolytic and Kinetic Characteristics of Maize Straw and the Seaweed Ulva pertusa," *Pyrolysis of Biomass*, vol. 5, no. 9, p. e12641, 2010.
[31] S. S. Kim, J. Kim, Y. H. Park, and Y. K. Park, "Pyrolysis Kinetics and Decomposition Characteristics of Pine Trees," *Bioresour. Technol*, vol. 101, no. 24, pp. 9797–9802, 2010.
[32] M. Becidan, Ø. Skreiberg, and J. E. Hustad, "Products Distribution and Gas Release in Pyrolysis of Thermally Thick Biomass Residues Samples," *J. Anal. Appl. Pyrolysis*, vol. 78, no. 1, pp. 207–213, 2007.
[33] M. M. Hagedorn and H. Bockhorn, "Pyrolytic behaviour of different biomasses (angiosperms) (maize plants, straws, and wood) in low temperature pyrolysis," *Journal of Analytical and Applied Pyrolysis*, vol. 79, pp. 136–146, 2007.
[34] T. Mani, P. Murugan, J. Abedi, and N. Mahinpey, "Pyrolysis of Wheat Straw in a Thermogravimetric Analyser: Effect of Particle Size and Heating Rate on Devolatilisation and Estimation of Global Kinetics," *Chem. Eng. Res*, vol. 478, pp. 1–7, 2010.
[35] R. Zanzi, K. Sjostrom, and E. Bjornbom, "Rapid Pyrolysis of Agricultural Residues at High Temperature," *Biomass Bioenergy*, vol. 23, pp. 357–366, 2002.
[36] A. Chouchene, M. Jeguirim, B. Khiari, F. Zagrouba, and G. Trouv é, "Thermal Devolatilisation of Olive Solid Waste: Influence of Particle Size and Oxygen Concentration," *Resour. Conserv. Recy*, vol. 54, pp. 271–277, 2010.
[37] T. G. Bridgeman, L. I. Darvel, J. M. Jones, P. T. Williams, R. Fahmi, A. V. Bridgwater, T. Barraclough, I. Shield, N. Yates, S. C. Thain, and I. S. Donnison, "Influence of Particle Size on the Analytical and Chemical Properties of Two Energy Crops," *Fuel*, vol. 86, pp. 60–72, 2007.
[38] E. Avni and R. W. Coughlin, "Kinetic analysis of lignin pyrolysis using nonisothermal TGA data," *Thermochimica Acta*, vol. 90, pp. 157-167, 1985.
[39] S. Pipatmanomai, N. Paterson, D. Dugwell, and R. Kandiyoti; "Kinetic Modeling of Coal Pyrolysis in an Atmospheric Wire-mesh Reactor," *The Joint International Conference on "Sustainable Energy and Environment (SEE)*, pp. 589- 594
[40] J. H. Flynn, and L. A. Wall, "A quick, direct method for the determination of activation energy from thermogravimetric data," J. Polym. Sci, Part B: Polym. Lett, vol. 4, pp. 323-328, 1966.
[41] Y. Tonbul and A. Saydut, "Thermal Behavior and Pyrolysis of Avgamasya Asphaltite," *Oil Shale*, vol. 24, no. 4, pp. 547–560, 2007.
[42] R. R. Keuleers, J. F. Janssens, and H. O. Desseyn, "Comparison of some methods for activation energy determination of thermal decomposition reactions by thermogravimetry," *Thermochimica Acta*, vol. 385, pp. 127–142, 2002.

Somayeh Daneshvar is a Ph.D. student in Marin System Engineering at the Osaka Prefecture University of Japan. She received her M.Sc. in Chemical Engineering from the same university.
Her current interest mainly lies in the area of developing a detailed understanding of hydrothermal and thermal conversion of variety biomass, evaluation the composition, and estimating the energy contents of biomass. She also works on bioenergy production from biomass as an alternative for fossil fuel.

Feridoun Salak obtained his Ph.D. in Chemical Engineering from the Osaka Prefecture University of Japan. His research interests lie predominately in the area of application of thermals and hydrothermal techniques for recovery of waste materials, particularly with respect to waste biomass hydrothermal conversion into value added chemicals and energy.
His current research works mainly included waste polymeric materials recovery and conversion into energy using (catalytic) pyrolysis technique. Dr. Salak is also doing research on hydrogen production by hydrolysis at higher temperatures as well.

Koji Otsuka obtained his Ph.D. in Naval Architecture from Osaka Prefecture University of Japan.
He is the professor at Department of Marine System Engineering of Osaka Prefecture University. He also deals with the project of environmental restoration in enclosed coastal area in Japan. Professor Otsuka is project manager of JICA Grassroots Project in Vietnam as well.
His related research interest lies in the area of feasibility study of deep ocean water (DOW) multiple utilization system, which consists of ocean thermal energy conversion using cold DOW and gasification of seaweed biomass.